

Term Project Part B -- Airfoil Simulation

Matthew Krist | Sully Nolan | Alexandria Smith | Sebastian Soldwisch | Christian Tello

2 March 2020

Colorado School of Mines

MEGN451 -- Section A

Professor Neal Sullivan

Introduction and Objectives

When a car reaches cruising speeds, the engine is using a majority of its power to counteract wind resistance which generally takes five times as much power than required to initially get the car moving from rest in the first place. With that being said, the more resistance or drag that can be reduced, the less the engine will have to work. This is where spoilers come in. Spoilers are implemented to disrupt airflow and in turn prevent lift on the car. Thus the vehicle can achieve negative lift and attain better traction to the roadway.

This project utilizes computational fluid dynamics to analyze how external airflow in a wind tunnel interacts with a Lamborghini Countach rear spoiler. Solidworks Flow Simulation was used to generate a variety of data that was found by changing the angle-of-attack of the spoiler. Nine studies were run, starting with an angle-of-attack of 0 degrees and ending with 30 degrees, increasing each study by an angle of 5 degrees. Additional studies were used at angles-of-attack at negative 30 degrees and negative 5 degrees to see how the results would compare despite it being very unlikely for these configurations to be used in industry. The simulations generated values for the drag force and lift force to also be used to calculate the lift coefficient and the drag coefficient of different angles-of-attack. This report includes detailed figures that show the variations in forces and coefficients in the nine studies.

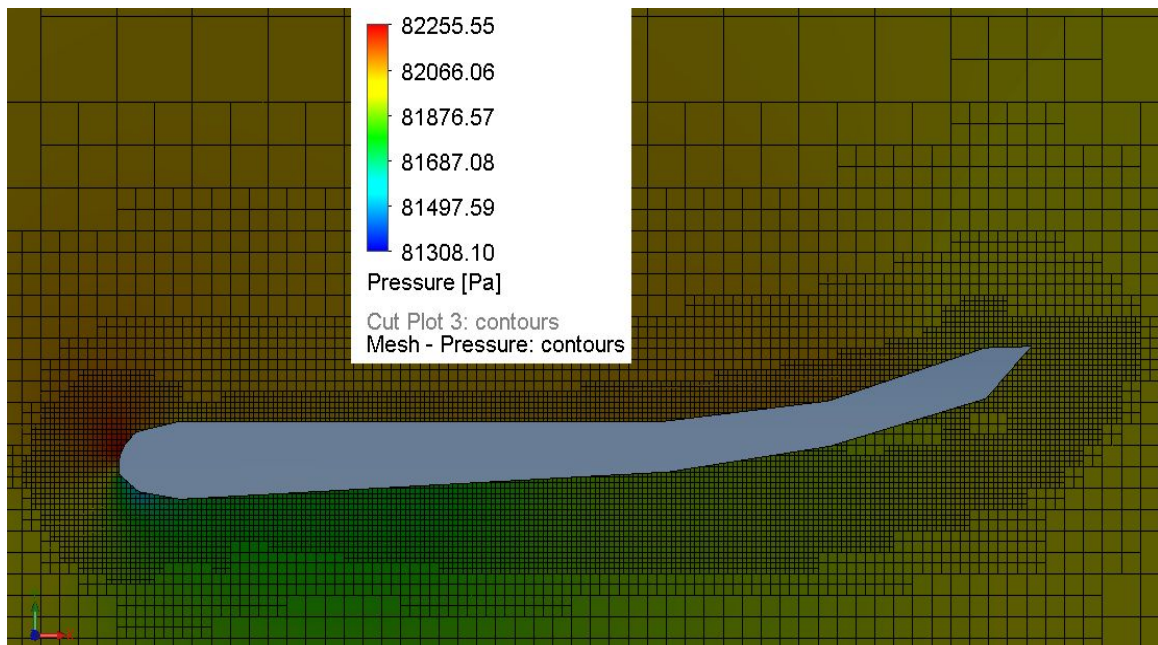


Figure 1: Airfoil with Meshing at Angle-of-Attack of 10 degrees

Results

The first portion of the analysis determined the lift and drag coefficients experienced by the spoiler, using Equations 1 and 2, when subjected to a 30 degree angle of attack and air flow at 50 mph.

$$F_L = C_L A_{spoiler} \left(\frac{\rho V^2}{2} \right) \quad \text{EQ.1}$$

$$F_D = C_D A_{spoiler} \left(\frac{\rho V^2}{2} \right) \quad \text{EQ.2}$$

Using these equations, the lift and drag coefficients were found to be 0.609 and 0.361 respectively. Continuing with this methodology, the series of simulations were conducted. The results from these studies can be observed in Figure 2.

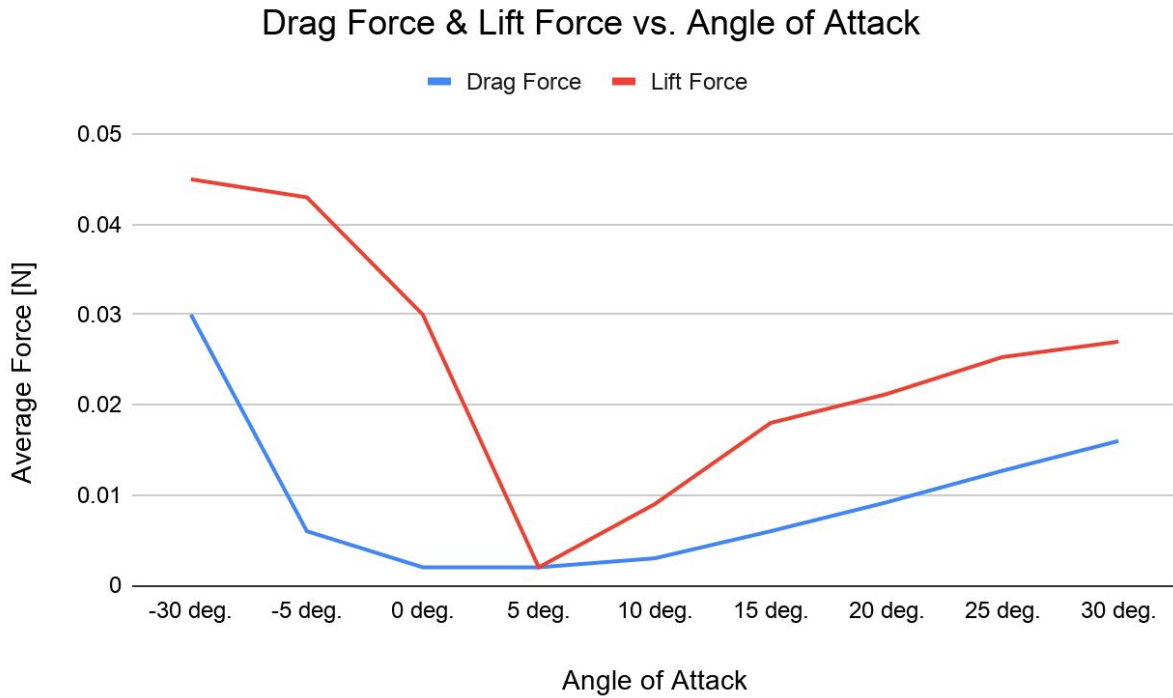


Figure 2: Plot of Drag and Lift Forces vs. Angle-of-Attack

Looking at Figure 2, it can be observed that the negative angles produced significantly higher drag and lift forces than positive values of the same angle. This is consistent with what the team expected to see and helps validate why negative angles-of-attack are not used in industry by automobile manufacturers. This figure also shows that the smallest forces occur at an angle-of-attack of 5 degrees. With these values obtained, the coefficients of lift and drag could be calculated and are plotted in the figure below.

Lift, Drag, & Ratio of Lift to Drag Coefficients vs. Angle of Attack

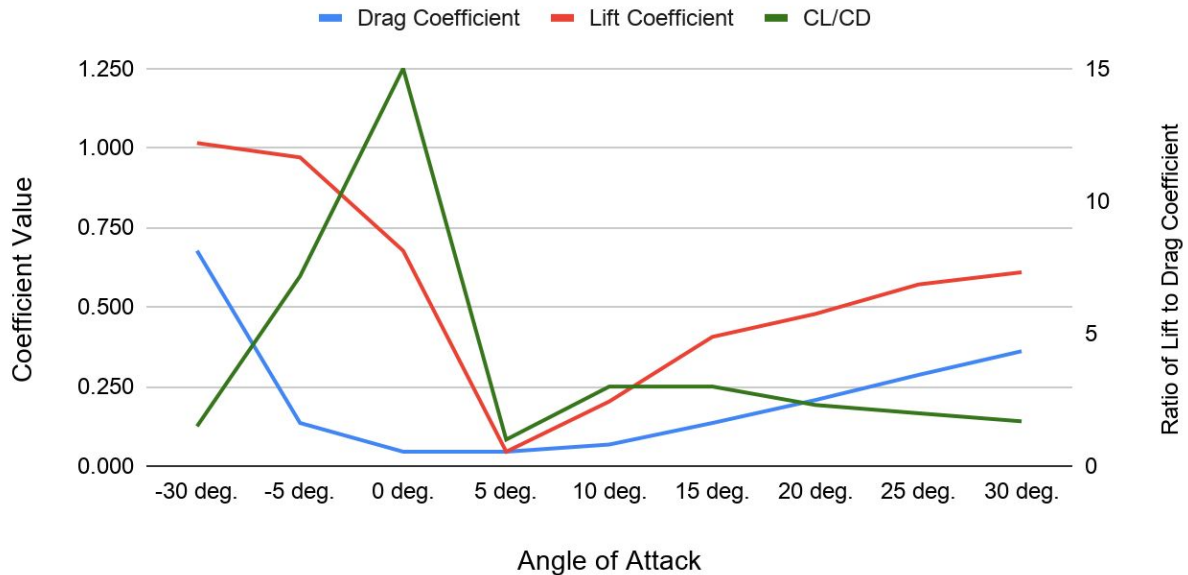


Figure 3: Plot of Drag Coefficient, Lift Coefficient, and Ratio of Lift Coefficient to Drag Coefficient vs. Angle-of-Attack

The results from Figure 3 reflect the poor performance that occurs with negative angles-of-attack that was seen in Figure 2. Comparing the results of drag coefficient to that of Fig. 11-39 from the course textbook, the magnitude of values are very similar, ranging from 0.0 to 0.4 and they have a similar exponential behavior as angle-of-attack increases. Additionally, the generated values for lift coefficients and can be compared to Fig. 11-44 that sees a dramatic increase in lift coefficient until 20 degrees. In the figure from the textbook, after this point, the curve decreases exponentially whereas the generated coefficient plot tends to flatten out but still increases. It is also worth noting that this part is shaped dramatically different than the conventional airfoil and these differences in performance would be expected with the design differences. Lastly, looking at how the ratio of lift to drag coefficients changes, the curve reaches its highest value at 0 degrees and the trend appears to level out as angle-of-attack increases.

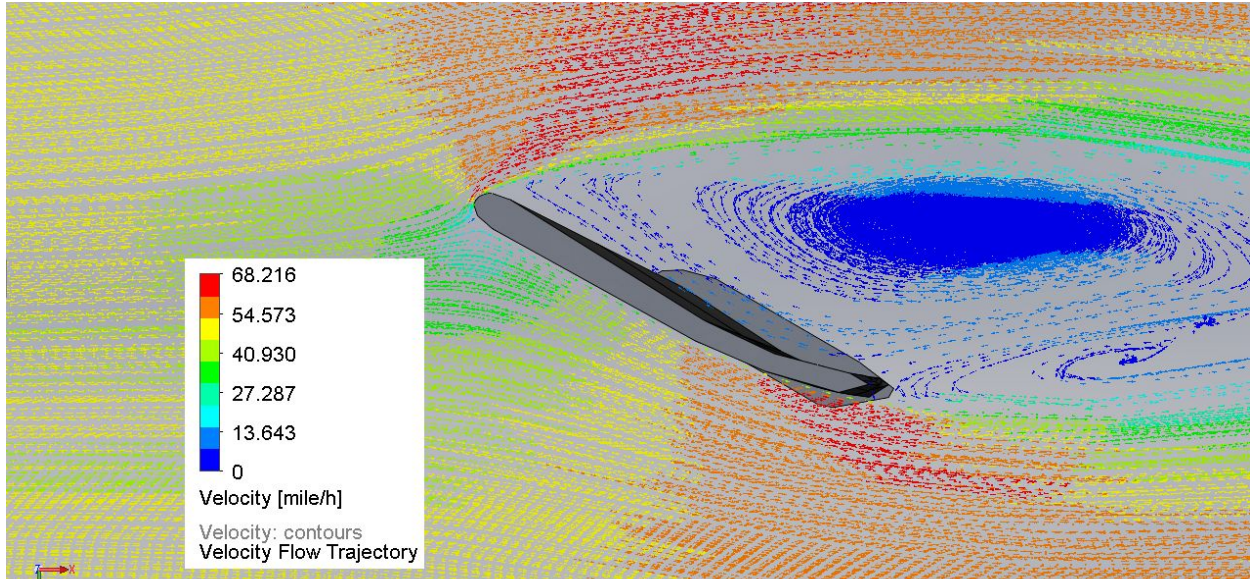


Figure 4: Original Simulation Velocity Flow Trajectory - 30 deg.

Above in Figure 4, significant turbulent flow is displayed above the airfoil's top surface. This turbulent flow can be attributed to the 30 degree angle of attack at which the air flows over the airfoil. In a real-life situation, this simulation would represent a non-optimal mounting of the Lamborghini Countach wing. Another flow structure present within Figure 4 is the vortex formation at the trailing edge of the airfoil. Certain areas of flow within the model may not represent real-world performance due to errors associated with simulation meshing. A finer mesh would result in more accurate simulation results.

The next portion of the analysis was to explore scaling and flow similarity between the real model spoiler and the prototype that was simulated. The assumptions and dimensions for both the model and the prototype are outlined in Table 1.

Characteristic	Model	Prototype
Air Density (kg/m ³)	1.225	0.97
Air Viscosity (kg/m/s)	1.789x10 ⁻⁵	1.789x10 ⁻⁵
Velocity (m/s)	22.35	To be calculated
Chord Length (m)	0.3556	.018288
Reynolds	5.44E+05	5.44E+05

Table 1: Model vs. Prototype Assumptions & Dimensions

$$Re_m = \frac{\rho_m V_m c_m}{\mu_m} = \frac{\rho_p V_p c_p}{\mu_p} = Re_p \quad \text{EQ. 3}$$

Using the values in Table 1 and the relation shown in Equation 3, the velocity needed to maintain the same Reynolds number between the prototype and model was found to be 1,227.6 mph. Although this number seems unlikely as no vehicle has ever reached a speed remotely close to this, due to the limitations in the variables that were able to be controlled in the simulation, this was the result that was scaled to be consistent with the Reynolds number similarity. As for the Mach number, the correlation was not applicable as both the model and simulated prototype are at sea level. Running a simulation that reflects the Reynolds-number similarity conditions at a velocity of 1,227.6 mph, the resulting values at an angle-of-attack of 30 degrees were drag force of 14.6 N and lift force = 24.6 N. These values are much higher than the original studies that were conducted as expected. Below, the velocity flow trajectory in Figure 5 displays turbulent flow on the top surface of the airfoil. Additionally, the flow separates from the top surface not long after making contact with the leading edge. In comparison to the standard velocity flow trajectory plot shown in Figure 4, the similarity study velocity flow trajectory plot exhibits a more immediate separation from the airfoil's top surface. Furthermore, the maximum plot velocity is larger than that of the original simulation. This increase in velocity impacts the behavior of the airflow over the airfoil, creating a turbulent region on the top side of the airfoil.

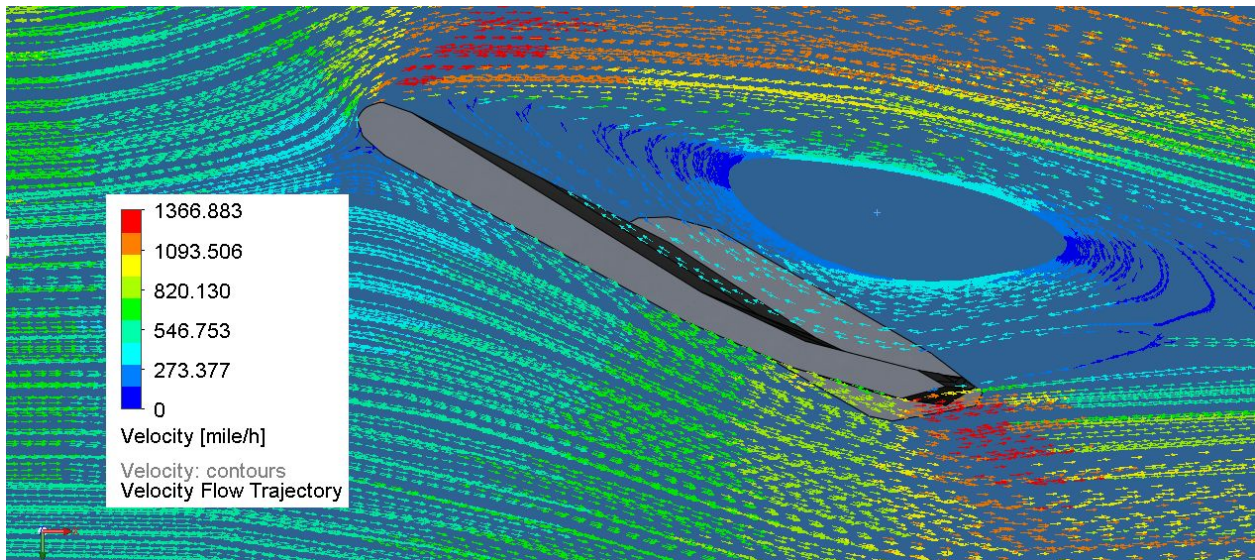


Figure 5: Similarity Study Velocity Flow Trajectory - 30 deg.